Inorganic Chemistry

Article

pubs.acs.org/IC

Computational Study of Metal−Dinitrogen Keggin-Type Polyoxometalate Complexes $[PW_{11}O_{39}M^{II}N_2)]^{5-}$ (M = Ru, Os, Re, Ir): Bonding Nature and Dinitrogen Splitting

Chun-Guang Liu,* Shuang Liu, and Ting Zheng

College of Chemical Engineering, Northeast Dianli University, No. 169 Changchun Road, Jilin City, 132012, P. R. China

Supporting Information

ABSTRACT: Molecular geometry, electronic structure, and metal−dinitrogen bonding nature of a series of metal−dinitrogen derivatives of Keggin-type polyoxometalates (POMs) $[PW_{11}O_{39}M^{II}N_2)]^{5-}$ (M = Ru, Os, Re, Ir) have been studied by using a density functional theory (DFT) method with the M06L functional. Among these Keggin-type POM complexes, Os- and Re-substituted POM complexes are the most active for N_2 adsorption with considerable adsorption energy. The electronic structure analysis shows that Os^{II} and Re^{II} centers in their metal−dinitrogen POM complexes possess $\pi^2_{xz}\pi^2_{yz}\pi^2_{xy}$ and $\pi^2_{xz}\pi^2_{yz}\pi^1_{xy}$ configurations, respectively. DFT-M06L calculations show that the possible synthesis routes proposed in this work for the Ru−, Os−, and Re−dinitrogen POM complexes are thermodynamically feasible under various solvent environments. Meanwhile, the Re−dinitrogen POM complex was assessed for the direct cleavage of dinitrogen molecule. In the reaction mechanism, a dimeric Keggin-type POM derivative of rhenium could represent the intermediate which undergoes N−N bond scission. The calculated free energy barrier ($\Delta G^{\ddagger}$) for a transition state with a zigzag conformation is 16.05 kcal mol^{-1} in tetrahydrofuran, which is a moderate barrier for the cleavage of the N−N bond when compared with the literature values. In conclusion, regarding the direct cleavage of the dinitrogen molecule, the findings would be very useful to guide the search for a potential N_2 cleavage compound into totally inorganic POM fields.

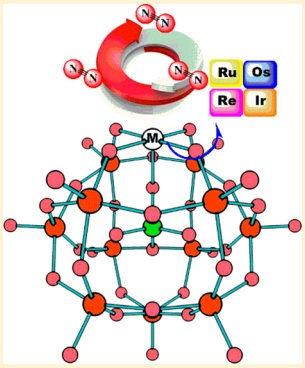

1. INTRODUCTION

Dinitrogen coordination chemistry is particularly important because of potential applications in the field of artificial nitrogen fixation.[1] During the past semicentury, many efforts have been made to characterize molecular geometry, physicochemical property, and electronic structure of transition metal dinitrogen complexes.[2] The nature of transition metal center and ancillary ligands is the key factor in determination of the metal−dinitrogen interaction. Research in this filed is strongly inspired by the nitrogenase enzyme, an iron−molybdenum−sulfur cluster.[3] A considerable amount of Fe− and Mo−dinitrogen complexes have been extensively investigated.[4] Simultaneously, Ru−, Os−, and Re−dinitrogen complexes, which belong to the same group in the periodic table of elements relevant to Fe and Mo elements, also have attracted considerable attention.[5]

Polyoxometalates (POMs) are early transition metal polynuclear oxo cluster. This class of inorganic compounds is unmatched not only in terms of remarkable structural diversity but also regarding reactivity and relevance to analytical chemistry, catalysis, medicine, and materials science.[6] POMs have the capability to stabilize most transition metal d electron centers through multiple μ-oxo bridging units. Moreover, it is to be expected that the unique electron-withdrawing nature of the POM ligand would be conducive to stabilize high-valent intermediates and assist protonation equilibria on the oxo surface. POMs incorporating transition metal ions, such as ruthenium,[7] osmium,[8] rhodium,[9] palladium,[10] and platinum,[11] etc., possess various structural types. Most of them are the monolacunary Keggin anions, which are prepared by treating discrete lacunary anions with appropriate complexation of the transition metal center.

A series of nitrido POM complexes $[PW_{11}O_{39}M^{VI}N]^{4-}$ (M = Ru, Re, Os) have been successfully synthesized and structurally characterized by Proust and co-workers.[12] The reactivity of a ruthenium−nitrido derivative $[PW_{11}O_{39}Ru^{VI}N]^{4-}$ has also been demonstrated.[12d] They found that $[PW_{11}O_{39}Ru^{VI}N]^{4-}$ can react with triphenylphosphane and has released the bis-(triphenylphosphane) iminium cation $[PPh_3{=}N{=}PPh_3]^{+}$ (Ph = phenyl) through several intermediates. All these interesting works shed light on the potential value of POM complexes in the field of artificial nitrogen fixation. However, an unambiguous identification and characterization of the POM-based dinitrogen complex is still a major challenge, owing to the inertness toward ligand exchange and purification issues. Very recently, promising data have been observed by Sokolov[13] et al. In their works, a ruthenium-containing POM $[PW_{11}O_{39}Ru^{II}NO]^{4-}$ has been synthesized for the first time in high yield by reaction of $[Ru(NO)Cl_5]^{2-}$ with monolacunary Keggin ligand, $[PW_{11}O_{39}]^{7-}$. In the reaction of $[PW_{11}O_{39}Ru^{II}NO]^{4-}$ with hydroxylamine, a ruthenium−dini-

Received: May 5, 2015
Published: August 4, 2015

DOI: 10.1021/acs.inorgchem.5b01002
Inorg. Chem. 2015, 54, 7929−7935

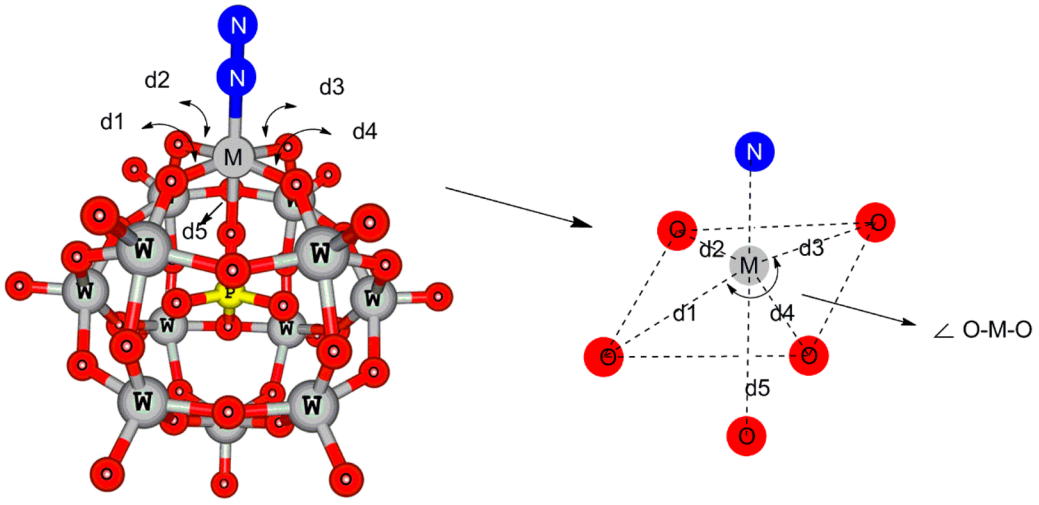

Figure 1. Molecular structure of metal−dinitrogen POM complexes.

trogen intermediate $[PW_{11}O_{39}Ru^{II}(N_2)]^{5-}$ has been detected according to ^{31}P NMR. Unfortunately, they failed to isolate this species. This dinitrogen POM complex finally aquates and oxidizes into $[PW_{11}O_{39}Ru^{III}H_2O]^{4-}$. Meanwhile, they were very careful about their determination based on only NMR data. Thus, electrospray ionization mass spectrometry was also employed for monitoring the reaction between $[PW_{11}O_{39}Ru^{II}NO]^{4-}$ and hydroxylamine. They successfully identified another ruthenium−dinitrogen POM complex $[PW_{11}O_{39}Ru^{III}(N_2)]^{4-}$, which is the oxidized species of $[PW_{11}O_{39}Ru^{II}(N_2)]^{5-}$. All their results provide strong evidence for the presence of ruthenium−dinitrogen POM complex $[PW_{11}O_{39}Ru^{II}(N_2)]^{5-}$.

It is intrinsically difficult to isolate the intermediate from mixtures of isostructural byproducts experimentally. In contrast, quantum chemistry calculations based on density functional theory (DFT)[14] are a useful tool to probe the nature of intermediate in POM chemistry. In the present paper, a systematic comparison of a Ru−dinitrogen POM complex and its Os, Re, and Ir analogues has been performed on the basis of DFT-M06L calculations. Such results provide a fundamental understanding of geometry, electronic structure, metal−dinitrogen bonding nature, and their relationships to the number of d electrons and oxidization state in the transition metal dinitrogen POM complexes.

2. COMPUTATIONAL DETAILS

All of the geometry optimizations were carried out using the DFT method with M06L functional[15] without any restriction on the symmetry. The 6-31G(d) basis set was used for the main group elements, and scalar relativistic effective core potential of LANL2DZ[16] was adopted for the metal elements. Vibrational frequencies were obtained at the same levels in this work. All of the structures discussed in the present work are minima or transition states on the corresponding potential energy surfaces, as confirmed by the correct number of imaginary frequencies. The adsorption energy (E_{ad}) of N_2 was calculated by

$$E_{ad} = E_{complex} - (E_{M-POM} + E_{N2})$$

where $E_{complex}$, E_{POM}, and E_{N2} are the total energies of the metal−dinitrogen POM complex, POM fragment, and N_2 molecule, respectively.

Bulk solvent effects of dichloromethane, tetrahydrofuran, and acetonitrile media have been taken into account via the self-consistent reaction field (SCRF) method, using the integral equation formalism polarizable continuum model (IEFPCM)[17] solvent model. The SMD solvation model[18] proposed by Truhlar and co-workers has been performed for computing ΔG of solvation. This model separates the solvation free energy into two main components. The first component is the bulk electrostatic contribution arising from being self-consistent with the solvent reaction field. The second component is the contribution arising from short-range interactions between the solute and solvent molecules in the first solvation shell. The SMD model has been proven effective for the treatment of neutral species,[18] ion species, and POMs[14a] with a small error in the solvation free energies computed by an appropriate basis set. Natural bond orbital (NBO) analysis[19] at the M06L/6-31G(d) level was performed to assign the atomic charges and Wiberg bond indices (WBI) (LANL2DZ basis sets on the metal atom). All calculations were implemented with the Gaussian 09 package.[20]

For transition-metal-substituted POM anions with high negative charge, it was not possible to consider the effects of a countercation with our computational resources. A lot of convincing cases indicate that the interesting physicochemical properties of POMs are mainly carried by the anion part. In the present paper, only the anion part has been employed to probe the dinitrogen coordination chemistry of POMs. We believe this procedure ensures that the fascinating physicochemical properties of these POMs studied here are not missed because of the unique coordination ability of these POM anions.

3. RESULTS AND DISCUSSION

The late transition metal complex always gives rise to a low-spin state. In the present Article, all metal−dinitrogen POM complexes studied here have been optimized at M06L/6-31G(d) levels (LANL2DZ basis sets on metal atom) in various spin states. According to our DFT calculations, all metal−dinitrogen POM complexes studied here are found to have a low-spin ground state (see Supporting Information Table S1).

In general, the interesting reaction chemistry of a transition metal complex is mainly due to a sterically hindered ligand environment around the transition metal center, which protects and stabilizes the reactive metal center.[5f,21] These metal−

DOI: 10.1021/acs.inorgchem.5b01002
Inorg. Chem. 2015, 54, 7929−7935

dinitrogen POM complexes studied here all contain the same lacunary Keggin-type ligand, $[PW_{11}O_{39}]^{7-}$, which contains a defect that is formed by four oxygen donor atoms and is always referred to as an "inorganic porphyrin-like" ligand. The difference between the lacunary POM and porphyrin ligands mainly arises from the geometric structure when they stabilize transition metal ions. For the porphyrin ligand, the metal ions lie close to the plane of the first coordination sphere. In contrast, the metal ions lay higher above the plane of the first coordination sphere in POM complexes (see Figure 1). The key geometric parameters of the series of metal−dinitrogen POM complexes obtained by DFT-M06L calculations have been listed in Table 1.

Table 1. Geometric Parameters (Bond Length in Å, Angles in Degree), Adsorption Energy (kcal mol^{-1}), and Partial Charges (e) on the Selected Atoms of the Metal−Dinitrogen POM Complexes, Where the Metal is Ru, Os, Re, and Ir

param	Ru−POM	Os−POM	Re−POM	Ir−POM
Geometric Parameters				
spin multiplicity	1	1	2	1
M−N	1.857	1.830	1.843	2.074
WBI(M−N)	0.995	1.149	1.220	0.634
N−N	1.145	1.157	1.168	1.149
WBI(N−N)	2.530	2.382	2.283	2.532
∠O−M−O	171	169	166	171
av M−O distance	2.070	2.049	2.034	2.060
N_2 adsorption energy	−44.37	−62.75	−61.28	−11.32
Partial Charges				
M	0.561	0.809	0.889	0.830
total charge of N_2	−0.093	−0.231	−0.357	−0.243
N1	0.090	0.020	−0.035	−0.085
N2	−0.183	−0.251	−0.322	−0.158
total charge of $[PW_{11}O_{39}]^{7-}$	−5.468	−5.578	−5.532	−5.587

Our DFT−optimized calculations show that the bond distance between the metal center and the four donor oxygen atoms (d_1, d_2, d_3, and d_4) is about 2 Å, and all transition metal centers were found to hang over the plane determined by the four oxygen donor atoms, reflecting an ∠O−M−O angle in the range 166−171° (see Table 1), which indicates that the transition metal center is in a pseudo-octahedral environment (see Figure 1). Compared with the standard octahedral structure, the significant distortion comes from the large bond distance between transition metal center and the O atom (d_5) of tetrahedral phosphate group PO_4^{3-}. This weakened bonding interaction provides an additional ability of the transition metal center to bind to a dinitrogen molecule (see Figure 1). According to our DFT calculations, Os− and Re−dinitrogen POM complexes possess a small ∠O−M−O angle (see Table 1), and thus a long M−O bond distance (d_5) relevant to others, which indicates that they should provide a strong metal−dinitrogen interaction. In order to check this molecular geometric prediction, the adsorption energy of dinitrogen over the POM complex has been calculated at M06L/6-31G(d) levels (LANL2DZ basis sets on metal atom). The calculated data have been listed in Table 1. It can be found that the adsorption energy of these metal−dinitrogen POM complexes increases in the following order: Os−POM < Re−POM < Ru−POM < Ir−POM. In particular, the Os− and Re−POMs possess considerable adsorption energy of −62.75 and −61.28 kcal mol^{-1}, respectively. This result is in good agreement with the prediction on the basis of their molecular geometries.

The bond distance depends on both the M−N interaction and the metal radius. The optimized metal−nitrogen bond distance decreases in the following order: Ir > Ru > Re > Os. The optimized N−N bond distance increases in the following order: Ru < Ir < Os < Re. The M−N and N−N distances are closely related to the metal−dinitrogen bonding nature. In the present paper, we also examine the bonding nature of those POM complexes by using NBO analysis. The calculated WBI value has been listed in Table 1. It can be found that the WBI values of the M−N bond decrease in the order Re (1.220) < Os (1.157) < Ir (1.149) < Ru (0.995), indicating the M−N single bond nature. Also, the WBI values of the N−N bond decrease in the order Ir (2.532) < Ru (2.530) < Os (2.382) < Re (2.283), confirming the weakened N−N triple bond nature. It is of considerable interest that the Re−dinitrogen POM complex has the largest M−N WBI value but the smallest N−N WBI value. The NBO partial charges of the metal−dinitrogen POM complexes are listed in Table 1. It can be found that the charge of the dinitrogen molecule in these POM complexes is negative. Compared with the neutral free nitrogen molecules, the negative charge on the dinitrogen moiety indicates the charge reorganization or transfer from the transition metal center to the coordinated dinitrogen molecule. We found that NBO partial charges of dinitrogen moiety increase in the following order: Re (−0.357) < Ir (−0.243) < Os (−0.231) < Ru (−0.093). This charge reorganization contributes to the activation of the dinitrogen molecule. Therefore, the Re−dinitrogen POM complex has the longest N−N distances and the smallest WBI value. Due to the considerable adsorption energy, we will focus on the Ru−, Os−, and Re−dinitrogen POM complexes in the following discussion.

IR spectroscopy is able to detect small structural differences and is a useful probe of the Keggin-type POM structure. In the present paper, the IR spectra of a series of metal−dinitrogen POM complexes have been calculated at M06L/6-31G(d) levels (LANL2DZ basis sets on metal atoms). In order to check the reliability of our DFT-derived results, we first reproduce the IR spectra of an known POM complex $[PW_{11}O_{39}Ru^{II}NO]^{4-}$, which have been reported by Sokolov et al.[13] It is well-known that the Keggin-type POM contains a cage of tungsten atoms linked by oxygen atoms with a tetrahedral phosphate group. Oxygen atoms form four physically distinct bonds (P—O_a, W—O_t, W—O_b—W, and W—O_c—W bonds), which have distinct infrared signatures: 1080 cm^{-1} for asymmetric stretch vibration of P−O_a (O_a corresponds to oxygen atom of tetrahedral phosphate group), 987 cm^{-1} for asymmetric stretch vibration of W═O_t (O_t corresponds to the terminal oxygen atoms), 890 cm^{-1} for bending vibration of W—O_b—W (O_b corresponds to oxygen atom bridging the two tungsten atoms), and 802 cm^{-1} for bending vibration of W—O_c—W (O_c represents oxygen atom at the corners of the Keggin structure). For the mono-transition-metal-substituted species, the triply degenerate P—O_a asymmetric stretch vibration (about 1080 cm^{-1}) of intact Keggin structure (α-$[PW_{12}O_{10}]^{3-}$) splits into two IR bands. Similar behavior is observed in several mono-transition-metal-substituted Keggin-type POM complexes.[22] Also, the W═O_t, W—O_b—W, and W—O_c—W vibrations are not significantly shifted when compared with that of the intact Keggin structure. Therefore, the five characteristic absorption peaks are easily employed to identify the structure

DOI: 10.1021/acs.inorgchem.5b01002
Inorg. Chem. 2015, 54, 7929−7935

Table 2. Calculated and Experimental Vibrational Frequencies (in cm^{-1}) and the Assigned Bands of the Series of POM Complexes Studied Here

	$[PW_{11}O_{39}Ru^{II}NO]^{4-}$					
model	expt	calcd	$[PW_{11}O_{39}Ru^{II}N_2]^{4-}$ calcd	$[PW_{11}O_{39}Os^{II}N_2]^{4-}$ calcd	$[PW_{11}O_{39}Re^{II}N_2]^{4-}$ calcd	assignment
ν_1	1091	1097	1075	1086	1072	$\nu(P-O_a)$
ν_2	1037	1025	1029	1025	1039	$\nu(P-O_a)$
ν_3	965	967	958	954	954	$\nu(W-O_t)$
ν_4	887	886	883	881	882	$\nu(W-O_b-W)$
ν_5	803	812	801	812	802	$\nu(W-O_c-W)$
ν_6	1850	1884	2116	2060	1980	$\nu(N-O)$ or $\nu(N-N)$

of mono-transition-metal-substituted Keggin-type POMs. According to FT−IR spectroscopy of $[PW_{11}O_{39}Ru^{II}NO]^{4-}$ reported in the literature,[13] the two P—O_a asymmetric stretch vibrations appear at 1091 and 1037 cm^{-1}, respectively; the W═O_t stretch vibrations, W—O_b—W, and W—O_c—W bending vibrations appear, respectively, at 965, 887, and 803 cm^{-1}. Also, a high-frequency and strong IR bond at 1850 cm^{-1} is assigned to the stretch vibrations of the coordinated NO^+ moiety. DFT-derived IR spectra have been compared in Table 2. It can be found that our DFT calculations reproduce these frequencies well. The largest difference between calculated and experimental frequencies is found to be the strong IR band at 1850 cm^{-1} corresponding to the stretch vibration of the N—O bond (1850 cm^{-1} (expt) vs 1884 cm^{-1} (calcd)).

For DFT-derived IR spectra of the ruthenium−dinitrogen POM complex, a significant change is found when it is compared with that of $[PW_{11}O_{39}Ru^{II}NO]^{4-}$. The IR band corresponding to P−O_a motion (ν_1) is predicted to shift by about 20 cm^{-1} upon replacement of NO^+ with N_2. Another distinct infrared signature is the absorption peak corresponding to the stretch vibrations of the N−N bond. The IR absorption band of free N_2(g) appears at 2331 cm^{-1} with a N−N bond length of 1.0975 Å. This frequency decreases with the elongation of the N−N bond.[1b] For example, azobenzene shows an IR band at 1442 cm^{-1} with the N−N bond length of 1.255 Å, and hydrazine shows an IR band at 1111 cm^{-1} with the N−N bond length of 1.460 Å. As mentioned above, the optimized N−N bond distance decreases in the order Re > Os > Ru in the series of metal−dinitrogen POM complexes. Our IR spectrum calculations reproduce this trend of N−N bond distance well. The calculated frequencies corresponding to the stretch vibrations of N−N bond increase in the order Re (1980 cm^{-1}) < Os (2060 cm^{-1}) < Ru (2116 cm^{-1}).

We employed the Os−dinitrogen POM complex as an example to analyze the electronic structure of those POM complexes. Because the Os^{II} center in POM ligand is in a pseudo-octahedral environment, the t_{2g} orbitals are not degenerate. The frontier molecular orbitals (FMOs) of this Os−dinitrogen POM complex are shown in Figure 2. It can be found that HOMO − 2 and HOMO − 1 orbitals are responsible for the metal−dinitrogen bonding interaction, and both orbitals are made from an overlap of the π^* orbital of the dinitrogen molecule with the symmetry adapted d_{xz} and d_{yz} orbitals of the Os^{II} center. On the basis of this orbital interaction, activation of the dinitrogen molecule in this metal−dinitrogen POM complex mainly comes from the donation of electron from the symmetry-adapted d_{xz} and d_{yz} orbitals of the Os^{II} center into molecular orbitals that are antibonding with respect to the dinitrogen molecule. For the d_{xy} orbital, it is destabilized by antibonding interactions with the p orbital of the four oxygen donor atoms. This raises this d_{xy}-like orbital energy level, reflecting the HOMO. The LUMO and its adjacent unoccupied orbitals are the symmetry-adapted combinations of the d-like orbital of the tungsten atom, which are not listed here. All results indicate that the Os^{II} center in this POM complex possesses a $\pi^2_{xz}\pi^2_{yz}\pi^2_{xy}$ configuration. In analogy, we determine that the Ru^{II} center in its POM complex has the same electronic configuration. Also, the Re^{II} center has a $\pi^2_{xz}\pi^2_{yz}\pi^1_{xy}$ configuration.

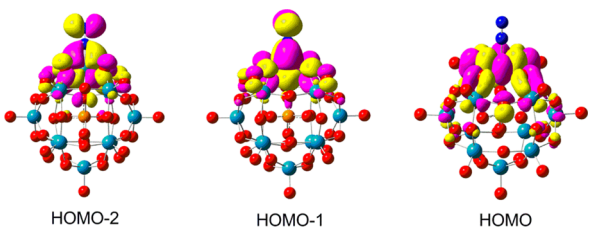

Figure 2. Frontier molecular orbitals of the Os−dinitrogen POM complex.

For late transition-metal-substituted Keggin-type POM anions, they always display a multistep reversible redox process. It is well-known that the redox property of a molecular system is closely associated with the nature of frontier molecular orbital. As shown in Figure 2, the HOMO − 2, HOMO − 1, and HOMO of $[PW_{11}O_{39}Os^{II}N_2]^{5-}$ are metal-based d orbitals of the Os^{II} center. Thus, a multistep redox process $Os^{II} \rightarrow Os^{III} \rightarrow Os^{IV} \rightarrow Os^{V}$ has been considered in this work. The HOMO of $[PW_{11}O_{39}Os^{II}N_2]^{5-}$ is the d_{xy}-like orbital of the Os^{II} center. Removal of an electron from this orbital would generate the one-electron-oxidized species with respect to $Os^{II} \rightarrow Os^{III}$ oxidized process. The optimized Os−N and N−N distances of the one-electron-oxidized species are listed in Table 3. It can be found that the Os^{III}−N distance increases to 1.854 Å ($\Delta r(Os^{II/III}-N)$ = 0.024 Å). Also, the N−N distance decreases to 1.038 Å ($\Delta r(N-N(Os^{II/III})$ = 0.012 Å). This indicates that the Os−N bond has been weakened and the N−N bond has been strengthened in this one-electron-oxidized process, but

Table 3. Geometric Parameters (Bond Length in Å, Angles in deg) of Various Osmium-Substituted POM Complexes

param	Os^{II}	Os^{III}	Os^{IV}	Os^{V}
Os−N	1.830	1.854	1.877	1.947
WBI(Os−N)	1.149	1.038	0.945	0.779
N−N	1.157	1.145	1.136	1.125
WBI(N−N)	2.382	2.490	2.586	2.714
∠Os−N−N	178	179	179	179
∠O−Os−O	169	172	173	171
av Os−O distance	2.049	2.011	1.957	1.921

DOI: 10.1021/acs.inorgchem.5b01002
Inorg. Chem. 2015, 54, 7929−7935

the changes are not substantial. This trend is mainly due to the ejected electron in the $Os^{II} \rightarrow Os^{III}$ oxidized process coming from a nonbonding d_{xy}-like orbital with respect to the M−N or N−N bonds. The FMO analysis of the Os^{III} species shows that the two metal-based d_{xz} and d_{yz} orbitals are doubly occupied and represent the bonding interaction between the Os^{III} center and dinitrogen molecule. Also, the metal-based d_{xy} orbital is singly occupied and nonbonding. This result supports that the Os^{III} center possesses a $\pi^2_{xz}\pi^2_{yz}\pi^1_{xy}$ configuration.

For the $Os^{III} \rightarrow Os^{IV}$ oxidized process, it would generate an Os^{IV} center with d^4 configuration. The DFT-M06L calculation shows that the Os^{IV} species possesses a singlet ground state. This indicates that the generation of the Os^{IV} species from the Os^{III} species arises from the ejection of an electron from the singly occupied d_{xy} orbital. The optimized Os−N and N−N distances of the Os^{IV} species are listed in Table 3. It can be found that the Os^{IV}−N bond increases to 1.877 Å, and the N−N bond distance decreases to 1.136 Å. The $\Delta r(Os^{III/IV}-N)$ and Δr(N−N) are, respectively, 0.023 and 0.009 Å (see Table 3), which indicates that the Os−N and N−N bonds are not significantly changed in a comparison with that of the Os^{III} species because the removal electron comes from the nonbonding d_{xy}-like orbital. The FMO analysis shows that the HOMO and HOMO − 1 of the Os^{IV} species are the doubly occupied d_{xz} and d_{yz} orbitals, which are representative of the Os^{VI}−N bonding interaction. All results indicate that the Os^{IV} center possesses a $\pi^2_{xz}\pi^2_{yz}\pi^0_{xy}$ configuration.

The $Os^{IV} \rightarrow Os^{V}$ oxidized process results in an Os^{V} center with a d^3 configuration. According to our DFT-M06L calculations, the Os^{V} species is found to have a low-spin ground state (doublet state). This indicates that the generation of Os^{V} species from Os^{IV} species arises from the ejection of an electron from the d_{yz}-like Os−N bonding orbital. The optimized calculation gives the Os^{V}−N bond distance of 1.947 Å (see Table 3), compared with the Os^{IV}−N bond length of 1.877 Å, which indicates that the $Os^{IV} \rightarrow Os^{V}$ oxidized process weakens the Os−N bond, $\Delta r(Os^{IV/V}-N)$ = 0.070 Å, which is larger than that of $Os^{II} \rightarrow Os^{III}$ and $Os^{III} \rightarrow Os^{IV}$ oxidized processes. This is mainly due to the removal electron coming from the Os−N bonding orbital.

All results indicate that the configuration of the Os center in this multistep redox process ($Os^{II} \rightarrow Os^{III} \rightarrow Os^{IV} \rightarrow Os^{V}$) can be assigned as $\pi^2_{xz}\pi^2_{yz}\pi^2_{xy} \rightarrow \pi^2_{xz}\pi^2_{yz}\pi^1_{xy} \rightarrow \pi^2_{xz}\pi^2_{yz}\pi^0_{xy} \rightarrow \pi^2_{xz}\pi^1_{yz}\pi^0_{xy}$. The calculated WBI values of Os−N bond in the series of oxidized processes decrease from 1.157 to 0.779 (see Table 3). This indicates that the Os−N bond in the series of oxidized processes is still the weak single bond. Also, the calculated WBI value of the N−N bond increases in the range 2.382−2.714 Å. The series of oxidized processes also affects other key geometry parameters, but these changes are not significant (see Table 3).

MacKay et al. proposed[1b] that the synthesis methods for transition metal−dinitrogen complexes can be roughly divided into three classes: (1) ligand substitution, replacement of a weakly bound ligand with dinitrogen, (2) spontaneous coordination of dinitrogen to a vacant site in the coordination sphere, and (3) reduction of transition metal complexes to low-valent species that bond and activate dinitrogen. In general, transition-metal-substituted Keggin-type POMs were synthesized by a direct reaction of discrete lacunary anion $[PW_{11}O_{39}]^{7-}$ with an appropriate transition metal complex. A number of transition-metal-substituted Keggin-type POM anions have been prepared by using this synthesis method,[6d] such as the ruthenium-substituted POMs, $[PW_{11}O_{39}Ru^{II}L]^{x-}$ (L = H_2O, DMSO, and NO^+).[13,23] With the above points taken into account, the ligand substitution may be a promising synthesis method for transition metal dinitrogen POM complexes.

We have calculated the free energy of the ligand-substituted reaction for the Ru−, Os−, and Re−POM complexes at room temperature and 1 bar pressure (see Table 4). The calculated

Table 4. Calculated $\Delta G_{298\ K}$ (kcal mol^{-1}) Values for the Ligand-Substituted Reactions in Dichloromethane, Acetonitrile, and Tetrahydrofuran Obtained by M06L/6-31G(d) Calculations (LANL2DZ Basis Sets for Metal Atom)

$[PW_{11}O_{39}M^{II}H_2O]^{5-} + N_2 = [PW_{11}O_{39}M^{II}N_2]^{5-} + H_2O$			
complex	dichloromethane	acetonitrile	tetrahydrofuran
Ru−POM	−15.40	−15.45	−15.77
Os−POM	−30.97	−30.92	−31.83
Re−POM	−32.91	−32.79	−34.59

$\Delta G_{298\ K}$ (kcal mol^{-1}) values show that, in dichloromethane, acetonitrile, and tetrahydrofuran, all reactions are thermodynamically allowed. Reactions of $[PW_{11}O_{39}Os^{II}H_2O]^{5-}$ and $[PW_{11}O_{39}Re^{II}H_2O]^{5-}$ with dinitrogen ($\Delta G_{298\ K}$ = ca. − 30 kcal/mol) are readily accessible relevant to the reaction of $[PW_{11}O_{39}Ru^{II}H_2O]^{5-}$ with dinitrogen ($\Delta G_{298\ K}$ = ca. − 15 kcal/mol). All results suggest that ligand substitution may be a feasible route thermodynamically for all three POM complexes studied here.

Another important event in dinitrogen chemistry is the cleavage of the N−N bond. Direct cleavage of the dinitrogen molecule by a linear bimetallic complex has been reported by Cummins and co-workers,[24] where a dinuclear molybdenum complex $[(R(Ar)N)_3Mo](\mu\text{-}N_2)[Mo(N(Ar)R)_3]$ (R = alkyl and Ar = 3, 5-$(CH_3)_2C_6H_3$) can undergo a first-order process of N−N bond cleavage via a rate-determining zigzag transition state. This direct-cleavage approach was expanded to our system and described in Scheme 1. The proposed mechanism in Scheme 1 contains two important intermediates, **2** and **3**. Coordination of the dinitrogen to the POM complex results in intermediate **2**, which has been systematically discussed above. Then, the second POM complex coordinates to **2**, which leads to the intermediate **3**, a dimeric Keggin-type POM complex (see Scheme 1).

In the present Article, dimeric Keggin-type POM complexes of ruthenium, osmium, and rhenium have been considered for direct cleavage of N—N bond. The molecular geometries of the series of dimeric Keggin-type POM complexes have been optimized by using M06L functional at 6-31G(d) levels (LANL2DZ basis sets on metal atom), and the key geometric parameters have been compared in Figure 3. It can be found that the metal−nitrogen bond distance decreases in the following order: Ru > Os > Re. The N—N distance increases in the following order: Ru < Os < Re. The most remarkable of these parameters is that of the dimeric Re complex, it has the largest N—N bond length. The Re atom in this complex is formally an oxidation state of +2 with one unpaired d electron, giving rise to two possible spin states, open-shell singlet state and triplet state. For the open-shell singlet state, the optimized calculations have been performed on the basis of broken-symmetry DFT method in this work. An effort to optimize the triplet state has not been achieved because of the significant geometric distortion of Re—N═N—Re unit. As shown in

DOI: 10.1021/acs.inorgchem.5b01002
Inorg. Chem. 2015, 54, 7929−7935

Scheme 1. Proposed Mechanism for the Cleavage of N−N bond[a]

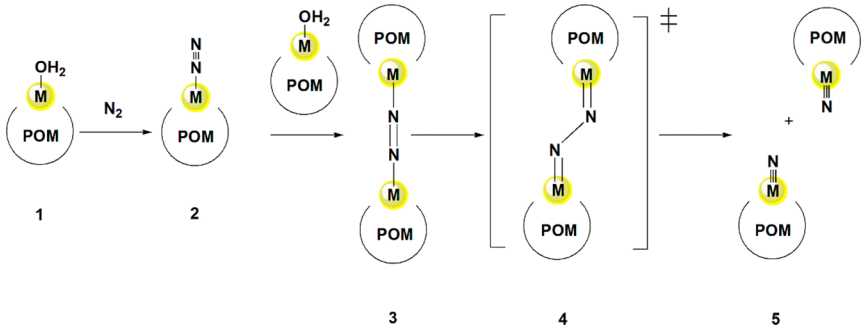

[a]A dimeric Keggin-type POM derivative of rhenium has been employed to probe this mechanism in the following discussion.

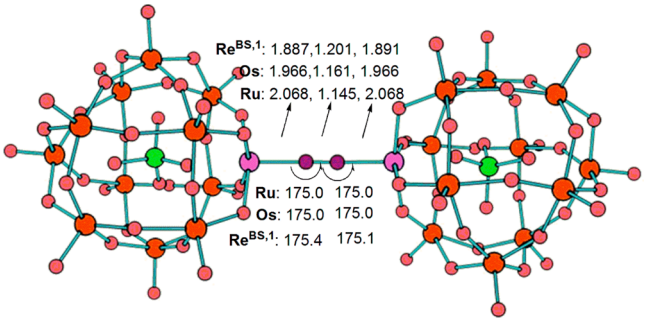

Figure 3. Optimized molecular structure of dimeric Keggin-type POM complexes of ruthenium, osmium, and rhenium (bond length in Å, angles in deg).

Figure 3, our DFT-M06L calculations show that the dimeric Re complex in the open-shell singlet state exhibits an almost linear Re—N═N—Re unit with the N—N bond distance of 1.201 Å, which is stretched by 0.03 Å from that in **2**.

According to our DFT-M06L calculations, the N−N bond cleavage of the dimeric Re complex in the open-shell single state takes place though a transition state **4** with a zigzag conformation at a moderate barrier, $\Delta G^{\ddagger}$ = 16.05 kcal mol^{-1} in tetrahydrofuran, and a N—N bond distance of 1.512 Å, which corresponds qualitatively to a N—N single bond. Schneider et al. recently reported[5a] that a dinuclear Re complex [(PNP)-ClRe(N_2)ReCl(PNP)] (PNP = N(CHCHPtBu_2)$_2$) can undergo the N—N cleavage via a zigzag transition state (N—N bond length is 1.64 Å) with a barrier, $\Delta G^{\ddagger}$ = ∼17.6 kcal mol^{-1} (84.4 kJ mol^{-1}), which is similar to our studied system. As shown in Figure 4, the cleavage of the dinitrogen molecule results in the formation of a nitrido POM complex **5** with a strong Re≡N triple bond. The overall reaction starting from the dimeric Re POM complex is exothermic by 39.09 kcal mol^{-1} in tetrahydrofuran. This suggests the thermodynamic driving force for the N—N cleavage reaction studied here.

4. CONCLUSION

DFT calculations have been performed to explore the molecular geometry, electronic structure, metal−dinitrogen bonding, IR spectroscopy, and possible synthesis methods for a series of metal−dinitrogen POM complexes $[PW_{11}O_{39}M^{II}(N_2)]^{5-}$ (M = Ru, Os, Re, Ir). Although all these POM complexes have a similar metal−dinitrogen moiety, their M−N and N−N distances are considerably different. According to the geometric structure and adsorption energy of the dinitrogen molecule over the POM complex, we found that

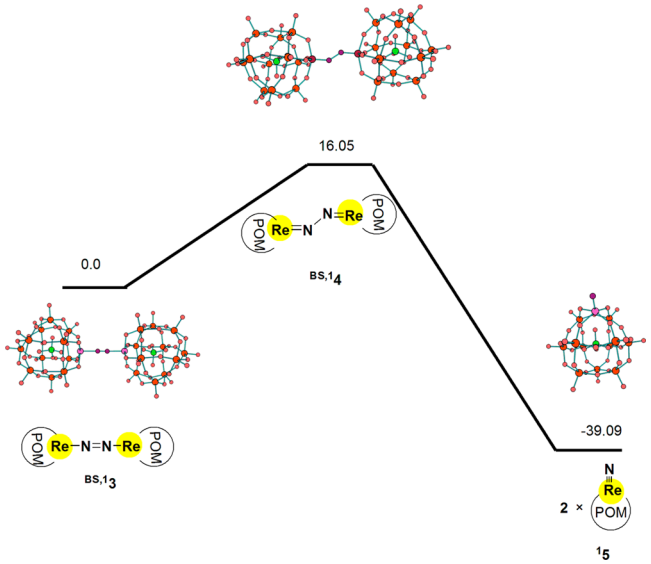

Figure 4. Calculated free energies for dinitrogen cleavage starting from the dimeric Re POM complex **3** in tetrahydrofuran (M06L/6-31G(d) calculations (LANL2DZ basis sets on metal atom)).

Os− and Re−dinitrogen POM complexes possess a strong metal−dinitrogen interaction. The WBI was employed to take the difference of ionic radii of metal centers into account, and we found that Re−dinitrogen POM complex has the largest M−N WBI value but the smallest N−N WBI value. The electronic structure analysis shows that Ru^{II} and Os^{II} centers in their metal−dinitrogen POM complexes both possess $\pi^2_{xz}\pi^2_{yz}\pi^2_{xy}$ configuration, and Re^{II} center has a $\pi^2_{xz}\pi^2_{yz}\pi^1_{xy}$ configuration. The electronic configuration of Os center in its multistep redox process can be assigned as $\pi^2_{xz}\pi^2_{yz}\pi^2_{xy} \rightarrow \pi^2_{xz}\pi^2_{yz}\pi^1_{xy} \rightarrow \pi^2_{xz}\pi^2_{yz}\pi^0_{xy} \rightarrow \pi^2_{xz}\pi^1_{yz}\pi^0_{xy}$. Compared with the experimental data, our DFT calculations reproduced the IR spectra of transition-metal-substituted Keggin-type POMs well. The characteristic absorption peaks of Ru−, Os− and Re−dinitrogen POM complexes have also been predicted on the basis of our DFT calculations. The possible synthesis routes of Ru−, Os−, and Re−dinitrogen POM complexes have also been proposed in this work. Our DFT calculations confirm that they are feasible routes thermodynamically for all three POM complexes studied here.

A dimeric Keggin-type POM complex of ruthenium could represent the intermediate which undergoes N−N bond scission. Our DFT calculations indicate that the cleavage of the N−N bond in this dimer takes place through a transition

DOI: 10.1021/acs.inorgchem.5b01002
Inorg. Chem. 2015, 54, 7929−7935

state with a zigzag conformation at a moderate barrier in tetrahydrofuran ($\Delta G^{\ddagger}$ = 16.05 kcal mol^{-1}). All of the reasonable relationships proposed in our work provide clear and good understanding of the interaction between the metal and the dinitrogen molecule and mechanism of N−N bond scission.

■ ASSOCIATED CONTENT

Supporting Information

Total energies of metal−dinitrogen POM complexes with various spin states based on M06L/6-31G(d)/LANL2DZ calculations. *xyz* coordinates for most relevant structures reported in this paper. The Supporting Information is available free of charge on the ACS Publications website at DOI: 10.1021/acs.inorgchem.5b01002.

(PDF)

■ AUTHOR INFORMATION

Corresponding Author

*E-mail: liucg407@163.com or liucg407@mail.nedu.edu.cn. Phone: 86 0432 64606919. Fax: 86 0432 64606919.

Notes

The authors declare no competing financial interest.

■ ACKNOWLEDGMENTS

The authors gratefully acknowledge the financial support from the National Natural Science Foundation of China (21373043).

■ REFERENCES

(1) (a) Jia, H. P.; Quadrelli, E. A. *Chem. Soc. Rev.* **2014**, *43*, 547−564. (b) MacKay, B. A.; Fryzuk, M. D. *Chem. Rev.* **2004**, *104*, 385−401.

(2) (a) Yandulov, D. V.; Schrock, R. R. *Science* **2003**, *301*, 76−78. (b) Arashiba, K.; Miyake, Y.; Nishibayashi, Y. *Nat. Chem.* **2011**, *3*, 120−125. (c) Anderson, J. S.; Rittle, J.; Peters, J. C. *Nature* **2013**, *501*, 84−87.

(3) (a) Allen, A. D.; Harris, R. O.; Loescher, B. R.; Stevens, J. R.; Whiteley, R. N. *Chem. Rev.* **1973**, *73*, 11−20. (b) Hoffman, B. M.; Lukoyanov, D.; Yang, Z. Y.; Dean, D. R.; Seefeldt, L. C. *Chem. Rev.* **2014**, *114*, 4041−4062.

(4) Hoffman, B. M.; Dean, D. R.; Seefeldt, L. C. *Acc. Chem. Res.* **2009**, *42*, 609−619.

(5) (a) Klopsch, I.; Finger, M.; Wutele, C.; Milde, B.; Werz, D. B.; Schneider, S. *J. Am. Chem. Soc.* **2014**, *136*, 6881−6883. (b) Khoenkhoen, N.; der Bruin, B.; Dzik, J. N. H. R. I. *Eur. J. Inorg. Chem.* **2015**, *2015*, 567−598. (c) Askevold, B.; Nieto, J. T.; Tussupbayev, S.; Diefenbach, M.; Herdtweck, E.; Holthausen, M. C.; Schneider, S. *Nat. Chem.* **2011**, *3*, 532−537. (d) Fedoseev, I. V.; Solov'ev, N. V. *Russ. J. Inorg. Chem.* **2007**, *52*, 994−995. (e) Allen, A. D.; Senoff, C. W. *Chem. Commun.* **1965**, 621−622. (f) Gilbert-Wilson, R.; Field, L. D.; Bhadbhade, M. *Inorg. Chem.* **2014**, *53*, 12469−12479. (g) Kunkely, H.; Vogler, A. *Angew. Chem., Int. Ed.* **2010**, *49*, 1591−1593.

(6) (a) Katsoulis, D. E. *Chem. Rev.* **1998**, *98*, 359−387. (b) Dolbecq, A.; Dumas, E.; Mayer, C. R.; Mialane, P. *Chem. Rev.* **2010**, *110*, 6009−6048. (c) Hill, C. L. *Chem. Rev.* **1998**, *98*, 1−2. (d) Izarova, N. V.; Pope, M. T.; Kortz, U. *Angew. Chem., Int. Ed.* **2012**, *51*, 2−21.

(7) (a) Khenkin, A. M.; Efremenko, I.; Weiner, L.; Martin, J. M. L.; Neumann, R. *Chem. - Eur. J.* **2010**, *16*, 1356−1364. (b) Bagno, A.; Bonchio, M.; Sartorel, A.; Scorrano, G. *Eur. J. Inorg. Chem.* **2000**, *2000*, 17−20. (c) Murakami, M.; Hong, D.; Suenobu, T.; Yamaguchi, S.; Ogura, T.; Fukuzimi, S. *J. Am. Chem. Soc.* **2011**, *133*, 11605−11613. (d) Geletii, Y. V.; Botar, B.; Kogerler, P.; Hillesheim, D. A.; Musaev, D. G.; Hill, C. L. *Angew. Chem., Int. Ed.* **2008**, *47*, 3896−3899. (e) Sartorel, A.; Carraro, M.; Scorrano, G.; de Zorzi, R.; Geremia, S.; McDaniel, N. D.; Bernhard, S.; Bonchio, M. *J. Am. Chem. Soc.* **2008**, *130*, 5006−5007.

(8) (a) Khenkin, A. M.; Shimon, L. J. W.; Neumann, R. *Inorg. Chem.* **2003**, *42*, 3331−3339. (b) Bi, L. H.; Li, B.; Wu, L. X.; Shao, K. Z.; Su, Z. M. *J. Solid State Chem.* **2009**, *182*, 83−88. (c) Laurencin, D.; Villanneau, R.; Gerard, H.; Proust, A. *J. Phys. Chem. A* **2006**, *110*, 6345−6355.

(9) (a) Wei, X.; Bachman, R. E.; Pope, M. T. *J. Am. Chem. Soc.* **1998**, *120*, 10248−10253. (b) Wei, X.; Dickman, M. H.; Pope, M. T. *J. Am. Chem. Soc.* **1998**, *120*, 10254−10255. (c) Wei, X.; Dickman, M. H.; Pope, M. T. *Inorg. Chem.* **1997**, *36*, 130−131. (d) Sokolov, M. N.; Adonin, S. A.; Sinkevich, P. L.; Vicent, C.; Mainichev, D. A.; Fedin, V. P. *Dalton Trans.* **2012**, *41*, 9889−9892.

(10) (a) Izarova, N. V.; Banerjee, A.; Kortz, U. *Inorg. Chem.* **2011**, *50*, 10379−10386. (b) Izarova, N. V.; Maksimovskaya, R. I.; Willbold, S.; Kogerler, P. *Inorg. Chem.* **2014**, *53*, 11778−11784.

(11) (a) Kato, M.; Kato, C. N. *Inorg. Chem. Commun.* **2011**, *14*, 982−985. (b) Kato, C. N.; Morii, Y.; Hattori, S.; Nakayama, R.; Makino, Y.; Uno, H. *Dalton Trans.* **2012**, *41*, 10021−10027.

(12) (a) Dablemont, C.; Hamaker, C. G.; Thouvenot, R.; Sojka, Z.; Che, M.; Maatta, E. A.; Proust, A. *Chem. - Eur. J.* **2006**, *12*, 9150−9160. (b) Kwen, H.; Tomlinson, S.; Maatta, E. A.; Dablemont, C.; Thouvenot, R.; Proust, A.; Gouzerh, P. *Chem. Commun.* **2002**, 2970−2971. (c) Besson, C.; Musaev, D. G.; Lahootun, V.; Cao, R.; Chamoreau, L.−M.; Villanneau, R.; Villain, F.; Thouvenot, R.; Geletii, Y. V.; Hill, C. L.; Proust, A. *Chem. - Eur. J.* **2009**, *15*, 10233−10243. (d) Lahootun, V.; Besson, C.; Villanneau, R.; Villain, F.; Chamoreau, L. M.; Boubekeur, K.; Blanchard, S.; Thouvenot, R.; Proust, A. *J. Am. Chem. Soc.* **2007**, *129*, 7127−7135.

(13) Sokolov, M. N.; Adonin, S. A.; Mainichev, D. A.; Sinkevich, P. L.; Vicent, C.; Kompankov, N. B.; Gushchin, A. L.; Nadolinny, V. A.; Fedin, V. P. *Inorg. Chem.* **2013**, *52*, 9675−9682.

(14) (a) Antonova, N. S.; Carbo, J. J.; Kortz, U.; Kholdeeva, O. A.; Poblet, J. M. *J. Am. Chem. Soc.* **2010**, *132*, 7488−7497. (b) Liu, C. G.; Yan, L. K.; Su, Z. M. *Dalton Trans.* **2011**, *40*, 2967−2974. (c) Liu, C. G.; Guan, W.; Yan, L. K.; Su, Z. M. *Eur. J. Inorg. Chem.* **2011**, *2011*, 489−494. (d) Liu, C. G.; Guan, W.; Yan, L. K.; Song, P.; Su, Z. M. *Dalton Trans.* **2009**, *38*, 6208−6213. (e) Liu, C. G.; Su, Z. M.; Guan, W.; Yan, L. K. *Inorg. Chem.* **2009**, *48*, 541−548. (f) Romo, S.; Antonova, N. S.; Carbo, J. J.; Poblet, J. M. *Dalton Trans.* **2008**, *37*, 5166−5172.

(15) Zhao, Y.; Truhlar, D. G. *J. Chem. Phys.* **2006**, *125*, 194101.

(16) (a) Hay, P. J.; Wadt, W. R. *J. Chem. Phys.* **1985**, *82*, 270−283. (b) Wadt, W. R.; Hay, P. J. *J. Chem. Phys.* **1985**, *82*, 284−293. (c) Hay, P. J.; Wadt, W. R. *J. Chem. Phys.* **1985**, *82*, 299−310.

(17) Tomasi, J.; Mennucci, B.; Cammi, R. *Chem. Rev.* **2005**, *105*, 2999−3093.

(18) Marenich, A. V.; Cramer, C. J.; Truhlar, D. G. *J. Phys. Chem. B* **2009**, *113*, 6378−6396.

(19) Glendening, A. E.; Carpenter, J. E.; Weinhold, F. *NBO Version 3.1*.

(20) Frisch, M. J.; Trucks, G. W.; Schlegel, H. B.; Scuseria, G. E.; Robb, M. A.; Cheeseman, J. R.; Scalmani, G.; Barone, V.; Mennucci, B.; Petersson, G. A.; et al. *Gaussian 09, Revision D.01*; Gaussian, Inc.: Wallingford, CT, 2009.

(21) (a) Laplaza, C. E.; Cummins, C. C. *Science* **1995**, *268*, 861−3. (b) Yandulov, D. V.; Schrock, R. R. *J. Am. Chem. Soc.* **2002**, *124*, 6252−6253. (c) Betley, T. A.; Peters, J. C. *J. Am. Chem. Soc.* **2004**, *126*, 6252−6254. (d) Fryzuk, M. D.; Johnson, S. A.; Patrick, B. O.; Albinati, A.; Mason, S. A.; Koetzle, T. F. *J. Am. Chem. Soc.* **2001**, *123*, 3960−3973. (e) Creutz, S. E.; Peters, J. C. *J. Am. Chem. Soc.* **2014**, *136*, 1105−1115. (g) Anderson, J. S.; Rittle, J.; Peters, J. C. *Nature* **2013**, *501*, 84−87.

(22) (a) Ho, R.; Klemperer, W. *J. Am. Chem. Soc.* **1978**, *100*, 6772−6774. (b) Dablemont, C.; Proust, A.; Thouvenot, R.; Afonso, C.; Fournier, F.; Tabet, J. C. *Inorg. Chem.* **2004**, *43*, 3514−3520. (c) Duhacek, J. C.; Duncan, C. D. *Inorg. Chem.* **2007**, *46*, 7253−7255.

(23) (a) Rong, C.; Pope, M. T. *J. Am. Chem. Soc.* **1992**, *114*, 2932−2938. (b) Rong, C. C.; So, H.; Pope, M. T. *Eur. J. Inorg. Chem.* **2009**, *2009*, 5211−5214.

(24) Laplaza, C. E.; Cummins, C. C. *Science* **1995**, *268*, 861−863.

DOI: 10.1021/acs.inorgchem.5b01002
Inorg. Chem. 2015, 54, 7929−7935